

# <sup>18</sup>F-FDG hybrid PET in patients with suspected spondylitis

S. Gratz<sup>1,2</sup>, J. Dörner<sup>3</sup>, U. Fischer<sup>4</sup>, T.M. Behr<sup>1,2</sup>, M. Béhé<sup>1,2</sup>, G. Altenvoerde<sup>2</sup>, J. Meller<sup>2</sup>, E. Grabbe<sup>4</sup>, W. Becker<sup>2</sup>

<sup>1</sup> Department of Nuclear Medicine, Philipps University of Marburg, Baldingerstraße, 35033 Marburg, Germany

<sup>2</sup> Department of Nuclear Medicine, Georg August University of Göttingen, Germany

<sup>3</sup> Department of Orthopedics, Georg August University of Göttingen, Germany

<sup>4</sup> Department of Radiology, Georg August University of Göttingen, Germany

Received 23 August and in revised form 11 November 2001 / Published online: 29 January 2002

© Springer-Verlag 2002

**Abstract.** This study investigated the value of fluorine-18 2'-deoxy-2-fluoro-D-glucose (FDG) imaging with a double-headed gamma camera operated in coincidence (hybrid PET) detection mode in patients with suspected spondylitis. Comparison was made with conventional nuclear medicine imaging modalities and magnetic resonance imaging (MRI). Sixteen patients with suspected spondylitis (nine male, seven female, mean age 59 years) prospectively underwent FDG hybrid PET (296 MBq) and MRI. For intra-individual comparison, the patients were also imaged with technetium-99m methylene diphosphonate (MDP) (555 MBq) ( $n=13$ ) and/or gallium-67 citrate (185 MBq) ( $n=11$ ). For FDG hybrid PET, two or three transverse scans were performed. Ratios of infected (target) to non-infected (background) (T/B) vertebral bodies were calculated. MR images were obtained of the region of interest. Patients found positive for spondylitis with MRI and/or FDG hybrid PET underwent surgical intervention and histological grading of the individual infected foci. Twelve out of 16 patients were found to be positive for spondylitis. Independent of the grade of infection and the location in the spine, all known infected vertebrae ( $n=23$ , 9 thoracic, 12 lumbar, 2 sacral) were detected by FDG hybrid PET. T/B ratios higher than  $1.45 \pm 0.05$  (at 1 h p.i.) were indicative of infectious disease, whereas ratios below this value were found in cases of degenerative change. FDG hybrid PET was superior to MRI in patients who had a history of surgery and suffered from a high-grade infection in combination with paravertebral abscess formation ( $n=2$ ; further computed tomography was needed) and in those with low-grade spondylitis ( $n=2$ , no oedema) or discitis ( $n=2$ , mild oedema). False-positive <sup>67</sup>Ga citrate images ( $n=5$ : 2 spondylodiscitis, 1 aortitis, 1 pleuritis, 1 pulmonary tuberculosis) and <sup>99m</sup>Tc-MDP SPET ( $n=4$ : 1 osteoporosis,

2 spondylodiscitis, 1 fracture) were equally well detected by FDG hybrid PET and MRI. No diagnostic problems were seen in the other patients ( $n=5$ ). In this study, FDG hybrid PET was superior to MRI, <sup>67</sup>Ga citrate and <sup>99m</sup>Tc-MDP, especially in patients with low-grade spondylitis (as compared with MRI), adjacent soft tissue infections (as compared with <sup>67</sup>Ga citrate) and advanced bone degeneration (as compared with <sup>99m</sup>Tc-MDP).

**Keywords:** Vertebral osteomyelitis – Activity – Bone – FDG hybrid PET

**Eur J Nucl Med (2002) 29:516–524**

DOI 10.1007/s00259-001-0719-8

## Introduction

The lack of specific clinical, laboratory and radiological findings in patients with a disease as potentially debilitating as infectious spondylitis is challenging. Biopsy will frequently need to be performed but is itself often non-diagnostic and not without risk. Therefore, identification of findings, often subtle, that strongly favour other entities in the differential diagnosis may be of equal clinical importance to findings suggestive of infection, particularly in the subset of patients who would otherwise be felt unlikely to have a disc space infection. Nuclear medicine studies such as bone scan or gallium-67 citrate imaging and magnetic resonance imaging (MRI) are complementary techniques and are often performed in combination [1, 2, 3, 4]. Because of unfavourable physical characteristics, <sup>67</sup>Ga citrate images, even when acquired using a single-photon emission tomographic (SPET) technique, cannot clearly define the local extension of infected spine lesions to adjacent bone or soft tissue structures – a problem which often has to be overcome by MRI of the region in question [4]. Since infectious spondylitis is characterised by the involvement of two adjacent vertebrae and the intervening disc, with se-

S. Gratz (✉)

Department of Nuclear Medicine, Philipps University of Marburg, Baldingerstraße, 35033 Marburg, Germany

e-mail: gratz@mail.uni-marburg.de

Tel.: +49-6421-2862815, Fax: +49-6421-67025

vere and early destruction of the end plates, a precise description of the number of infected vertebrae and the extension of infection (assuming it is indeed present) is an urgent requirement [5].

Fluorine-18 2'-deoxy-2-fluoro-D-glucose (FDG) positron emission tomography (dedicated PET) has demonstrated high sensitivity and specificity in detecting and identifying processes of inflammatory activity in spondylitis. This technique has the advantage of higher spatial resolution as compared with other nuclear medicine procedures. In addition, it can differentiate between bone and soft tissue infection and allows imaging in the presence of metal implants [6, 7].

Recently, we presented our results obtained with FDG imaging using a double-head coincidence camera (hybrid PET) in patients with fever of unknown origin (FUO), in comparison with  $^{67}\text{Ga}$  citrate planar and SPET imaging [8]. The better performance of FDG as compared with  $^{67}\text{Ga}$  citrate was believed to be due to two factors: (a) the better spatial resolution of the hybrid PET system in comparison with a conventional gamma camera and (b) the tracer kinetics of the small FDG molecule as compared with the relatively large  $^{67}\text{Ga}$  citrate complex [8]. This new gamma camera system, capable of operating in a coincidence mode, is now viewed as a low-cost alternative to dedicated PET systems. The clinical impact of different double-head coincidence cameras (hybrid PET) in comparison with dedicated PET (dPET) systems is currently under investigation. So far, most experience has been gained with FDG imaging in malignant diseases [9, 10, 11]; little experience exists in the field of FDG imaging of infectious and/or degenerative changes.

Therefore, the aim of this study was to prospectively evaluate the performance of FDG using a hybrid PET system in patients with suspected spondylitis and to compare the results with those of conventional nuclear medicine imaging modalities (bone scan,  $^{67}\text{Ga}$  citrate SPET) and MRI. Patients with suspected spinal malignancies were strictly excluded from the study. Particular interest was instead focussed on the uptake of FDG in vertebral bodies showing degenerative changes (osteochondrosis, osteophytes etc.) and the adjacent facet joints (spondylarthrosis).

## Materials and methods

### Study design

This prospective, comparative study was approved by the Institutional Ethics Committee and informed consent was obtained from the participants. Sixteen patients with suspected spondylitis (nine males, seven females, mean age 59 years, range 25–78 years) were referred to the nuclear medicine department of the Georg August University of Göttingen for infection scanning (between June 1999 and December 2000). FDG hybrid PET and MRI were performed first, and  $^{67}\text{Ga}$  citrate or bone scan was performed 24 h later. Twelve patients were suspected of having vertebral osteomy-

elitis, three had been referred because of suspected spondylodiscitis and one had suffered postoperative bacteraemia. The patients had been on antibiotics for  $6\pm 5$  weeks prior to scanning.

The scintigraphic results were verified by the following procedures: fine-needle aspiration ( $n=7$ ), culture of a sample, obtained surgically ( $n=6$ ), histological examination (including the grading of infection) of a biopsy specimen ( $n=6$ ), MRI ( $n=16$ ), bone scan ( $n=13$ ) and  $^{67}\text{Ga}$  citrate scan ( $n=11$ ). Follow-up proved the presence of signs or symptoms of infection in patients with positive scintigraphic findings, or a favourable response to treatment.

### Imaging protocol and image interpretation

**FDG hybrid PET.** Imaging with FDG was performed after an overnight fast. The serum glucose levels were measured in all patients and were below 100 mg/dl. List-mode acquisition was started 1 h after injection of 296 MBq FDG using a double-head coincidence camera (Prism 2000 XP, Marconi Medical Systems, Espelkamp, Germany). The intrinsic resolution of this system before reconstruction is 5 mm transaxially. We used axial septa and photopeak to photopeak acquisition for whole-body and transaxial tomographic imaging.

For transaxial imaging of the cervical, thoracic, abdominal and pelvic regions, the acquisition involved the rotation of each detector over  $180^\circ$  with 30 stops and an acquisition time of 70 s for the first angle. After rebinning the raw data, transaxial tomographic images were generated using an iterative algorithm (ISA) [12].

**Bone scans.** In a first step, three-phase bone scintigraphy was performed after injection of 555 MBq technetium-99m methylene diphosphonate ( $^{99\text{m}}\text{Tc}$ -MDP). Immediately after bolus injection, dynamic images (1 image/s over 60 s) were acquired with a single-head gamma camera [Prism 100, Marconi Medical Systems (formerly Picker) Cleveland, Ohio, USA]. Subsequently, static blood pool images (1 image/120 s) of the region of interest were generated with a double-headed whole-body gamma camera (Prism 2000, Marconi Medical Systems, Cleveland, Ohio, USA). Whole-body bone scans were performed with a parallel-hole high-resolution, low-energy (HR) collimator using the 140-keV  $^{99\text{m}}\text{Tc}$  peak, a  $256\times 256$  matrix and a preselected time of 25 min/image.

For SPET data acquisition of  $^{99\text{m}}\text{Tc}$ -MDP bone scans, we employed a triple-headed gamma camera (Prism 3000, Marconi Medical Systems, Cleveland, Ohio, USA), a  $256\times 256$  matrix with a preselected time of 25 min/image, 30 images/ $120^\circ$ , and a parallel-hole high-resolution, low-energy collimator using the 140-keV  $^{99\text{m}}\text{Tc}$  peak. For SPET reconstruction, the same iterative algorithm (ISA) as mentioned above was applied [12].

**Gallium-67 citrate scans.** Gallium-67 citrate imaging was performed 2–3 days after FDG hybrid PET, and 48 h after i.v. injection of 185 MBq  $^{67}\text{Ga}$  citrate. Both whole-body scans (Prism 2000, Marconi Medical Systems, Cleveland, Ohio, USA) and SPET images (Prism 3000, Marconi Medical Systems, Cleveland, Ohio, USA) were acquired. For whole-body imaging, a  $64\times 64$  matrix with a preselected time of 25 min/image and a medium-energy collimator using the 93-, 185- and 300-keV photopeaks were employed. For SPET data acquisition, the same gamma camera with a  $64\times 64$  matrix, 30 images/ $120^\circ$ , 25 s/stop and the same medium-energy collimator were used. For SPET reconstruction, the same iterative algorithm (ISA) was applied [12].

**Image interpretation.** Images were interpreted separately by two independent observers who were blinded to the results of the verification procedures. Disagreements were settled by consensus. Scans were considered positive for infection when there was focal accumulation of tracer that increased over time. A scan was regarded as false positive when the abnormal uptake was misleading in the diagnosis. A true-negative scan was a normal study following which further evaluation excluded focal inflammation. A scan was considered false negative when no abnormal uptake was seen but focal inflammation was subsequently detected by other modalities. For quantitative evaluation, radiotracer uptake by the diseased vertebral bodies was measured. For this purpose, regions of interest (ROIs) over two suspicious adjacent vertebral bodies were compared with identically sized ROIs over two normal adjacent vertebral bodies. The results were correlated with histological findings and with the localisation in the spine. The count rates were classified as normal (equal to adjacent normal vertebral body), increased or decreased.

**MRI.** Images were obtained with T1-weighted and T2-weighted spin-echo (SE) pulse sequences. Plain or contrast-enhanced sagittal (for bony structures) and transverse (for paravertebral abscesses) studies were performed. Fat saturation was also applied [13, 14, 15]. Infection was considered to be present on MRI if (a) T1-weighted sequences showed confluent decreased signal intensities of the vertebral marrow and intervertebral disc space together with absence of a discernible margin between the disc and the adjacent vertebral marrow, (b) T2-weighted sequences documented an increased signal intensity of the vertebral marrow adjacent to the involved disc and of the disc itself and (c) significant contrast enhancement could be seen around the discovertebral junction and in the paravertebral soft tissues.

#### Statistical analysis

For statistical analysis, which was performed on the basis of the individual infected foci, the paired Student's *t* test was used. The level of significance was set at 0.05.

## Results

A summary of the patients, their scintigraphic results and the verification procedures is provided in Table 1. Examples of abnormal FDG hybrid PET, <sup>67</sup>Ga citrate scans and bone scans (SPET) are shown in Figs. 1, 2, 3 and 4. In patients with medium- and high-grade spondylitis, the results of FDG hybrid PET and MRI were 100% concordant. No focal infections (on FDG hybrid PET) or infectious lesions of single vertebrae (on MRI) were missed by either technique. Of the 16 patients, 12 had proven infection in the spine. Positive fine-needle biopsy, histology and culture were obtained in 7/12 patients found positive for infection. In the remaining five patients, biopsy results were unavailable. Out of 31 suspicious vertebrae, 23 (9 thoracic, 12 lumbar and 2 sacral) were found to be positive for infection.

With FDG hybrid PET a clear distinction was possible between infections of single vertebrae and adjacent soft tissue, whereas equivocal results were often seen with the other imaging modalities. An extensive paravertebral soft tissue abscess (*n*=1) (Fig. 1) was not seen with MRI or bone scan. FDG hybrid PET showed acute spon-

**Table 1.** Summary of all patients with suspected vertebral osteomyelitis and the results of FDG hybrid PET, bone scan (<sup>99m</sup>Tc-MDP SPET), <sup>67</sup>Ga citrate scan and MRI

Patient	Age (years)	Sex	FDG hybrid PET	Bone scan	<sup>67</sup> Ga citrate SPET	MRI	Final diagnosis	Verified by:
1	55	m	TP	FN	Equivocal	TP	Pleuritis	CT, MRI
2	63	f	TP	FN	Equivocal	TP	Aortitis	MRI, CL
3	62	f	TP	TP	TP	TP	Spondylitis	FN, CT
4	63	m	TP	FP	FP	Equivocal	Spondylodiscitis	H, CT, FN
5	58	m	TN	FP	TP	TN	Osteoporotic fracture	Op
6	54	f	TP	TP	TP	TP	Spondylitis	CT, H
7	58	m	TP	TP	ND	TP	Spondylitis	CT, CL, FN
			+ paraver. abs.	+FN			+ paraver. abs.	
8	49	f	FP	FP	TN	TP	Fracture	CT
9	63	m	TP	ND	TP	Equivocal	Spondylitis	H, CT
10	68	f	TP	FP	FP	Equivocal	Spondylodiscitis	CL, H, CT, FN
11	56	m	TP	TP	ND	TP	Spondylitis	CT, CL
			+ paraver. abs.	+FN			+ paraver. abs.	
12	61	f	TP	ND	TP	TP	Spondylitis	CL
13	69	m	TP	ND	ND	Equivocal	Spondylitis	FN, H
14	70	f	TP	TP	ND	Equivocal	Spondylitis	FN, H
15	58	m	TP	TP	TP	Spondylitis	Spondylitis	CT, CL
			+ infected scar	+FN	-	+ equivocal		
16	54	m	TP	TP	ND	TP	Spondylitis	FN, CT

TP, True positive; TN, true negative; FP, false positive; FN, false negative; ND, not done; CL, culture; FN, fine needle; H, histology; Op, operation

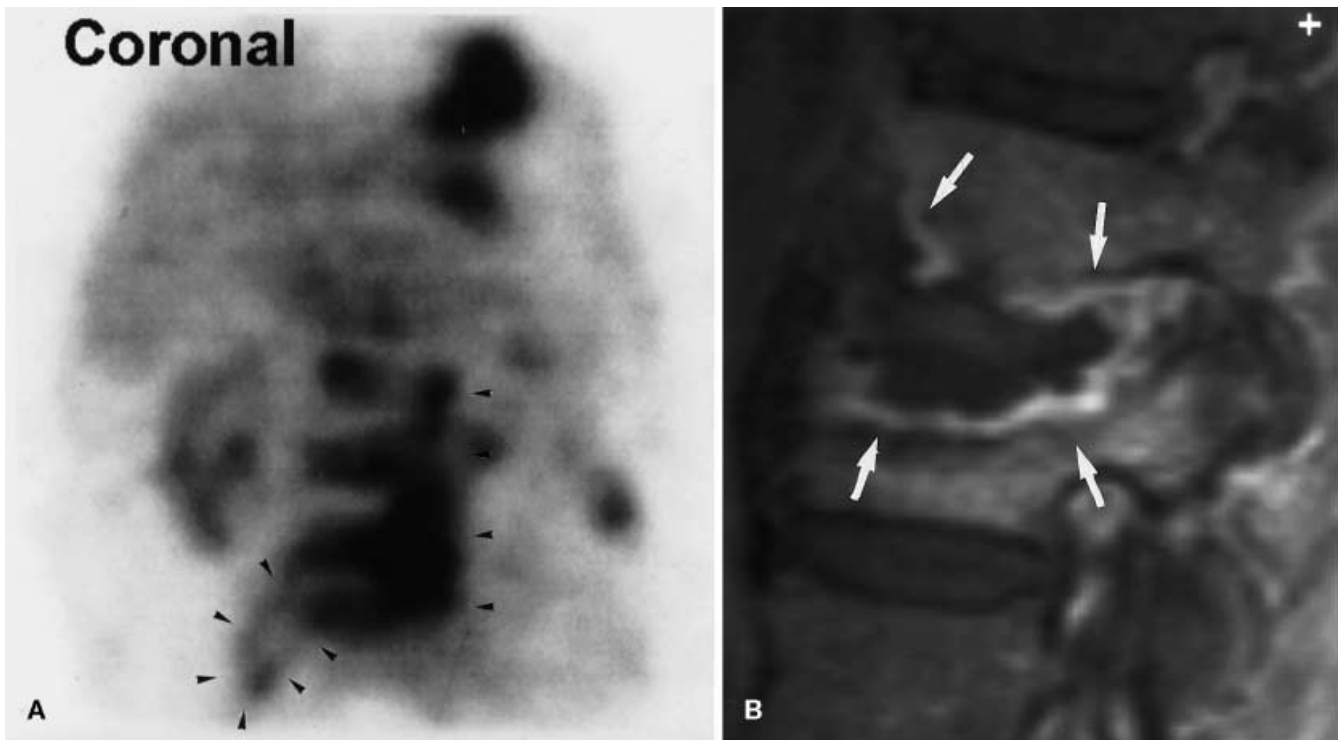


**Fig. 1.** FDG hybrid PET (A) allows an estimation of the number of infected vertebrae (*thin arrowheads*) as well as an estimation of the infection of the surrounding soft tissue (*thin arrowheads*). With MRI (B), the grade of infection was correctly shown (strong oedema, *thick arrows*), whereas the soft tissue abscess formation was not observed

dylitis in four lumbar vertebrae and further soft tissue abscess formation in the right psoas and inguinal region. Retrospective repeated evaluation of MRI still did not reveal a positive result in respect of the soft tissue infection, and further contrast-enhanced computed tomography (CT) was needed for final diagnostic confirmation. Infected scar tissue at the site of previous surgery ( $n=1$ ) (Fig. 2), smaller soft tissue infections adjacent to lumbar vertebrae ( $n=1$ ) and infections of intervertebral discs ( $n=2$ ) (Fig. 3) were all correctly interpreted with FDG hybrid PET. By contrast, both  $^{67}\text{Ga}$  citrate and  $^{99\text{m}}\text{Tc}$ -MDP SPET scans led to misclassifications as positive for spondylitis. The lower physiological resolution of  $^{67}\text{Ga}$  citrate did not allow correct differentiation between these anatomical structures. Soft tissue abnormalities were missed with  $^{99\text{m}}\text{Tc}$ -MDP and with MRI in patients with low-grade spondylodiscitis (mild oedema).

A false-positive result was obtained with hybrid PET in one of two patients with bone fractures. Hybrid PET showed slightly increased FDG uptake (Fig. 4), misclassified as positive for spondylitis. No signs of infectious disease were seen on MRI (no oedema), and treatment was deferred. The final diagnosis was made on the basis of MRI/CT. Other degenerative bone alterations such as

spondylophytes and osteochondrosis always showed decreased FDG uptake.

With MRI, false-negative results were obtained in four patients with spondylodiscitis ( $n=2$ ) and low-grade spondylitis ( $n=2$ , histologically proven). Due to the presence of small amounts of oedema in the peri-osseous soft tissue, MRI could not differentiate between mild osteomyelitis, activated osteoarthritis (there was one false-positive case on MRI) and advanced degeneration. Conventional radiography, which has limited reliability in cases of low-grade infection, showed no bone alterations indicative of infection. CT of the region of interest was also not indicative for infection, because there was little or no contrast enhancement. The final diagnosis was reached on the basis of the good response of the patient to antibiotic chemotherapy and the regression of leukocytosis.

The sensitivity, specificity and diagnostic accuracy for FDG hybrid PET, MRI,  $^{67}\text{Ga}$  citrate and bone scan were, respectively, 100%/87%/96%, 82%/85%/81%, 73%/61%/80% and 91%/50%/80%.

Outside the spine, FDG hybrid PET detected two cases of infected decubitus, one abdominal abscess, one infected operative site, one case of aortitis, one case of pleuritis, one case of pulmonary tuberculosis and two paravertebral abscesses. In four of these cases,  $^{67}\text{Ga}$  citrate SPET could not differentiate between soft tissue infection alone and concurrent infection of adjacent bone. Once detected, the extent of the lesion was much better delineated by FDG hybrid PET and MRI.

For FDG hybrid PET, the T/B (infection/normal vertebra) ratio was  $1.45 \pm 0.05$  at 1 h p.i., which was lower

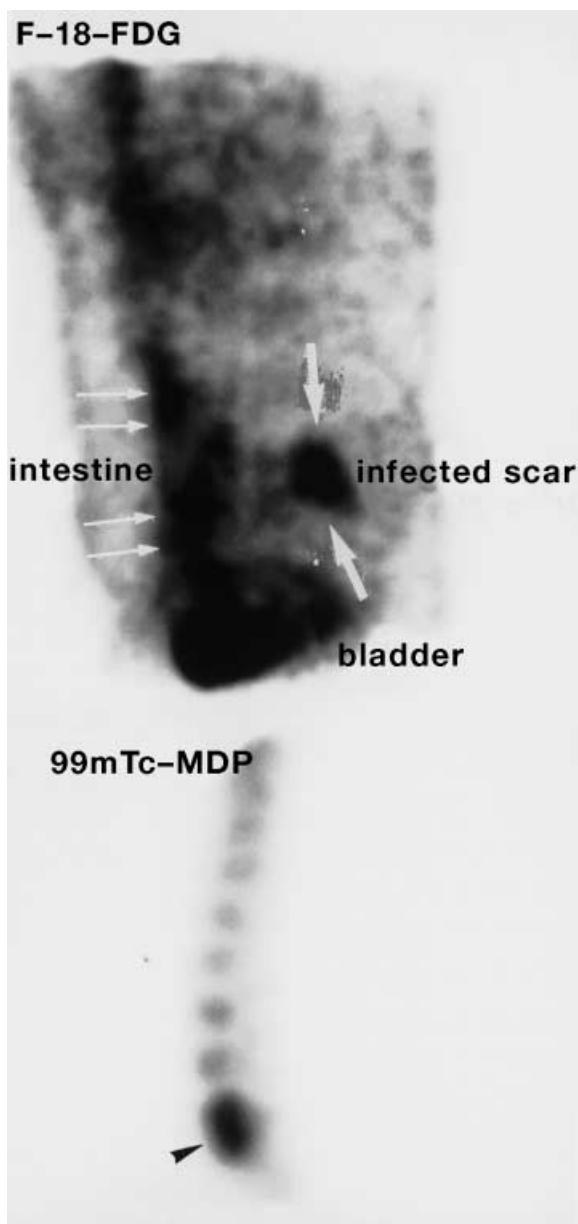


**Fig. 2.** Due to better spatial resolution, FDG allows clear differentiation between bone and surrounding soft tissue infection (*upper figure*, two arrows around the infected scar), whereas bone scan alone only shows the infected vertebra (*lower figure*, arrowhead). Radiologically disturbing artefacts, such as postoperative metal clips in the soft tissue (operative site), do not affect FDG imaging

than the ratios on  $^{67}\text{Ga}$  citrate SPET at 48 h p.i. ( $1.76 \pm 0.07$ ) and  $^{99\text{m}}\text{Tc}$ -MDP SPET at 4 h p.i. ( $2.34 \pm 0.25$ ). The uptake on FDG hybrid PET and  $^{67}\text{Ga}$  citrate SPET correlated with the severity of infection, whereas no correlation could be found for  $^{99\text{m}}\text{Tc}$ -MDP SPET since bone fractures, infections of bone structures and advanced bone alterations equally showed increased uptake. The paired *t* test showed no significant difference between the T/B ratios of FDG hybrid PET and  $^{67}\text{Ga}$  citrate SPET ( $P=0.41$ )

## Discussion

Spinal osteomyelitis has been known about for centuries. The advent of MRI has proved a major milestone; with its high sensitivity and specificity, it is an essential part of the diagnostic work-up. The treatment of spinal osteomyelitis follows the same basic principles as that for any infection. Once the diagnosis has been established, early conservative treatment is commenced. MRI shows signs of infection (bone marrow oedema), which is an early but rather unspecific finding. In advanced stages, however, CT is of benefit owing to the commonness of osseous lesions and the regression of bone marrow oedema. For this reason, both methods have to be used in a complementary manner in the differential diagnosis of acute and/or chronic spondylitis [17].

Recently, FDG PET has been proven to be very reliable in excluding osteomyelitis when a negative scan result is obtained. Overall, FDG PET correctly diagnosed the presence or absence of chronic osteomyelitis in 20 of 22 patients. Six had chronic osteomyelitis and 16 proved to be free of osteomyelitis. FDG PET correctly identified all six patients with chronic osteomyelitis but produced two false-positive results. This study had a sensitivity of 100%, a specificity of 87.5% and an accuracy of 90.9% [18]. An improvement in specificity could be achieved when FDG PET was focussed on patients with suspected infection of the central skeleton: the sensitivity was then 100%, the specificity 90% and the accuracy 94% [19]. In a direct comparison, FDG PET proved superior to MRI in infected bone areas with diminished vascularity, such as infection of a fibular transplant, which was missed by MRI [20]. A similar situation of diminished vascularity has to be expected in patients with suspected spondylitis, especially when they are under antibiotic chemotherapy prior to imaging [4]. This represents a frequent and clinically relevant situation. In the present study, laboratory findings such as WBC, ESR and CRP were only moderately increased in most patients. It remains unclear whether these findings were due to the encapsulation of the infection with a subsequent rise in pressure and a decrease in the vascular egress of necrotic cells [21] or whether they were just due to the local antibiotic response.

This study indicates that FDG hybrid PET performs as well as MRI in patients with high- and medium-grade infection of the central locomotor system. The infections were mainly localised in the thoracic and lumbar parts of the spine. Both methods depicted all 23 vertebrae known to be positive for infection, including chronic infections and infections limited to the intervertebral disc. The specificity of 85% with MRI reflects its limitations in detecting low-grade infections or inflammation limited to the intervertebral disc. In four patients, non-enhanced and enhanced STIR or fat-saturated sequences did not reveal the marrow abnormality (oedema) or its extension,

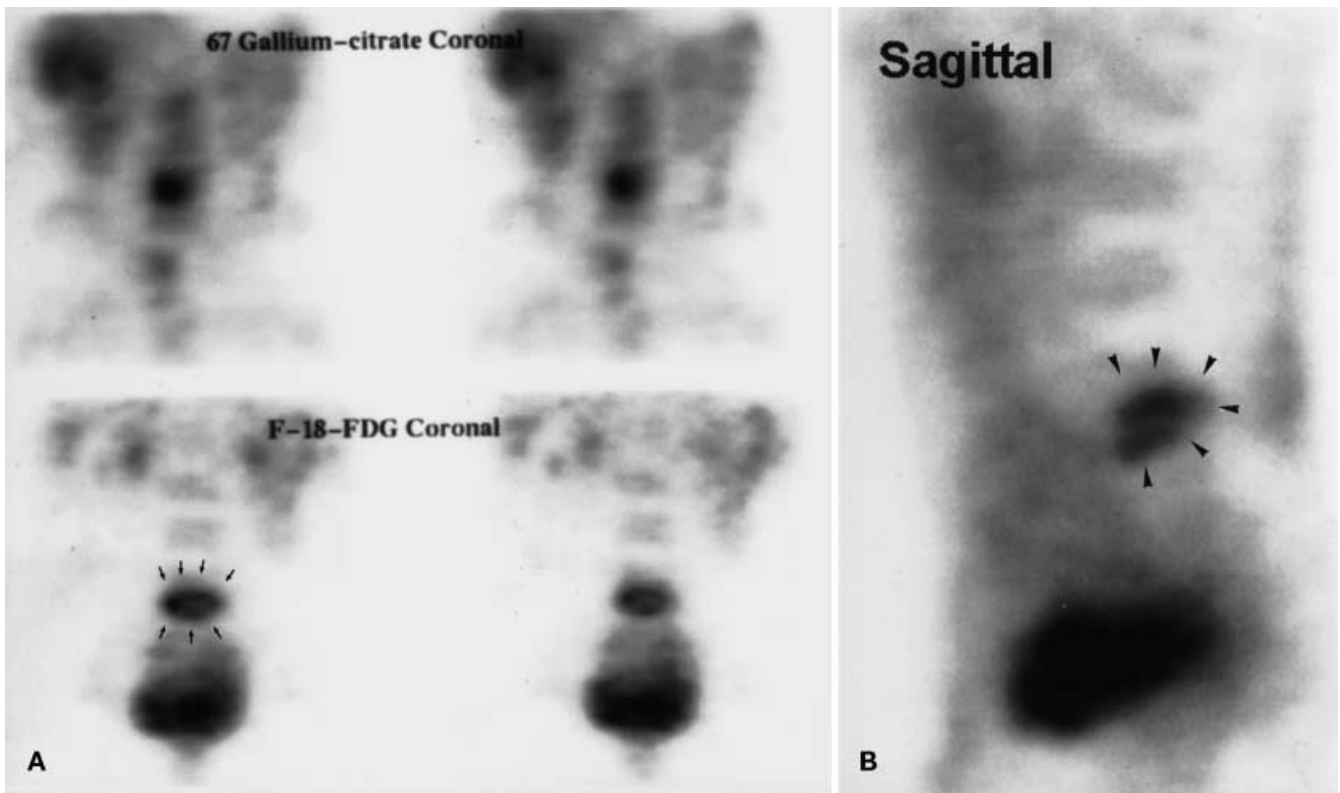


**Fig. 3A, B.** With FDG, spondylodiscitis is visualised as a rim sign (A, arrows around the infection on coronal slices, lower part of figure; B, arrowheads on the sagittal slice).  $^{67}\text{Ga}$  citrate (A, arrow on coronal SPET, upper part of figure) cannot differentiate between an infection limited to the intervertebral disc and an infection extending into the adjacent vertebrae

as has already been described elsewhere [4, 5, 22]. By contrast, no problems were encountered with FDG hybrid PET, because low numbers of inflammatory cells, such as neutrophils and activated macrophages, that are present in areas of acute and chronic inflammation avidly take up FDG [23, 24, 25] owing to increased glycolytic activity. The most important results of our study are that FDG hybrid PET is highly accurate and superior to the other imaging modalities:

1. In diagnosing acute and chronic spondylitis, because normal bone marrow shows only low glucose metabolism under physiological conditions [26] and decreased glucose uptake in the presence of degenerative bone alterations, such as osteochondrosis/osteophytes and osteoporotic demineralisation. However, slightly increased uptake of FDG was observed in one patient with a recent post-traumatic fracture of a lumbar vertebra, this being responsible for the only misclassification on FDG hybrid PET.
2. In differentiating between bone infection and infection of the surrounding soft tissue. In contrast, MRI misclassified two patients with paravertebral soft tissue

and scar infection as negative and  $^{67}\text{Ga}$  citrate SPET yielded a false-positive diagnosis for spondylitis in one case of aortitis, one of pleuritis and one of pulmonary tuberculosis. In contrast, clear differentiation between osteomyelitis and infection of the surrounding soft tissue was possible with FDG hybrid PET owing to the high spatial resolution of this new technique.

With dedicated PET, Kälicke et al. [27] and Guhlmann et al. [26] have already shown the advantage of functional imaging over CT and MRI, since metal implants in the bone did not affect imaging quality. In our study, two patients with a postoperative infection of the operative site (and metal clips) could not be adequately diagnosed with MRI. FDG hybrid PET was the only imaging procedure to elucidate the extension of infection.

Dedicated PET with FDG has proven to be an important diagnostic tool in oncology [28] as well as in patients with bone infections [26, 27]. However, the high cost of dedicated PET limits its use to a few, highly specialised institutions. For this reason, gamma camera manufacturers have adapted their relatively inexpensive double-head gamma cameras to perform PET imaging (hybrid PET). In this study, FDG hybrid PET correctly identified 12 of the 16 suspected infections of the central skeleton. There was only one indeterminate finding concerning a recent fracture of a vertebra, a result that most likely was related to the intensive bone repair of the intra-osseous fracture. In patients with fracture non-unions, it is well known that diagnosis of

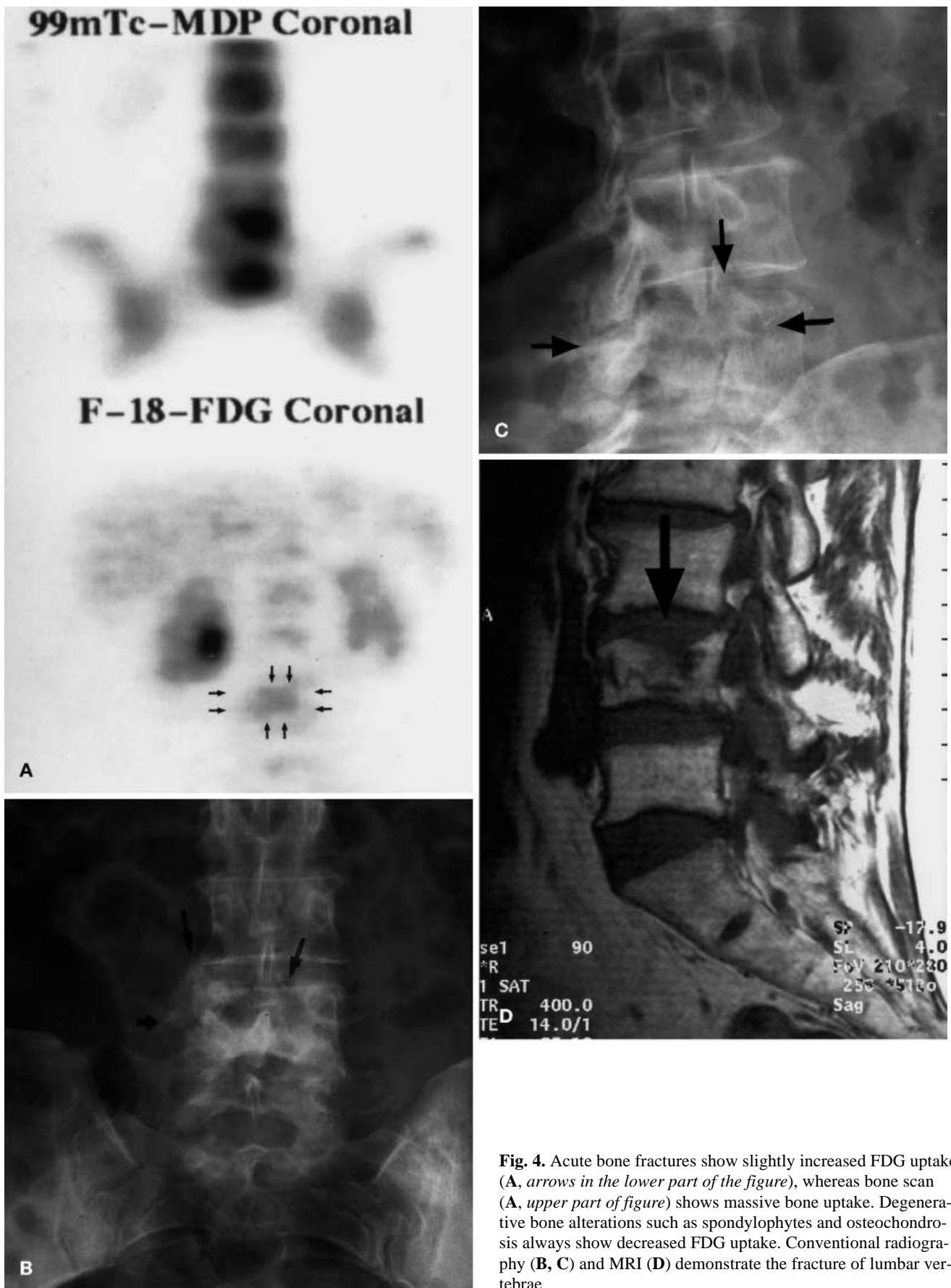


**Fig. 4.** Acute bone fractures show slightly increased FDG uptake (A, arrows in the lower part of the figure), whereas bone scan (A, upper part of figure) shows massive bone uptake. Degenerative bone alterations such as spondylophytes and osteochondrosis always show decreased FDG uptake. Conventional radiography (B, C) and MRI (D) demonstrate the fracture of lumbar vertebrae

osteomyelitis may be difficult with bone scan and/or gallium scintigraphy, because increased bone remodeling can lead to false-positive results [29]. It has been reported that the sensitivity, specificity and diagnostic accuracy of dedicated PET in patients with infections of the central skeleton are 100%, 90% and 94%, respectively [19]; corresponding figures for hybrid PET in our study were 100%, 87% and 96%. Both methods are superior to the other nuclear medicine and radiological methods. To our knowledge, this is the first time that the new technique of hybrid PET has demonstrated diagnostic values as high as those achieved with dedicated PET.

In summary, FDG hybrid PET helps to correctly identify those patients with vertebral osteomyelitis. It aids in the differentiation between mild infection and degenerative changes, detects additional manifestations outside the spine in a substantial number of patients and shows a good correlation with the histological severity of infection. The ease of use, excellent imaging quality and diagnostic accuracy make FDG hybrid PET an attractive and cost-effective imaging modality for more widespread clinical use.

## References

1. Adatepe MH, Powell OM, Isaacs GH, Nichols K, Cefola R. Hematogenous pyogenic vertebral osteomyelitis: diagnostic value of radionuclide bone imaging. *J Nucl Med* 1986; 27:1680–1685.
2. Lew DP, Waldvogel FA. Osteomyelitis. *N Engl J Med* 1997; 336:999–1007.
3. Palestro CJ, Torres MA. Radionuclide imaging in orthopedic infections. *Semin Nucl Med* 1997; 27:334–345.
4. Gratz S, Dörner J, Oestmann JW, Opitz M, Behr T, Meller J, Grabbe E, Becker W. <sup>67</sup>Ga-citrate and <sup>99</sup>Tc<sup>m</sup>-MDP for estimating the severity of vertebral osteomyelitis. *Nucl Med Commun* 2000; 21:111–1120.
5. Stabler A, Reiser MF. Imaging of spinal infection. *Radiol Clin North Am* 2001; 39:115–135.
6. Schmitz A, Källicke T, Willkomm P, Grünwald F, Kandyba J, Schmitt O. Use of fluorine-18 fluoro-2-deoxy-D-glucose positron emission tomography in assessing the process of tuberculous spondylitis. *J Spinal Disord* 2000; 13:541–544.
7. Vanninen E, Laitinen T, Partanen K, Tulla H, Herno A, Kroger H. Late correlative imaging findings of previous acute infective spondylitis. *Clin Nucl Med* 2000; 25:779–784.
8. Meller J, Altenvoerde G, Munzel U, Jauho A, Behe M, Gratz S, Luig H, Becker W. Fever of unknown origin: prospective comparison of [<sup>18</sup>F]FDG imaging with a double-head coincidence camera and gallium-67 citrate SPET. *Eur J Nucl Med* 2000; 27:1617–1625.
9. Weber WA, Neverve J, Sklarek J, Ziegler SI, Bartenstein P, King B, Treumann T, Enterrottacher A, Krapf M, Haussinger KE, Lichte H, Prauer HW, Thetter O, Schwaiger M. Imaging of lung cancer with fluorine-18 fluorodeoxyglucose: comparison of a double-head gamma camera in coincidence mode with a full-ring positron emission tomography system. *Eur J Nucl Med* 1999; 26:388–395.
10. Tatsumi M, Yutani K, Watanabe Y, Miyoshi S, Tomiyama N, Johkoh T, Kusuoka H, Nakamura H, Nishimura T. Feasibility of fluorodeoxyglucose double-head gamma camera coincidence imaging in the evaluation of lung cancer: comparison with FDG PET. *J Nucl Med* 1999; 40:566–573.
11. Abdel-Dayem HM, Radin AI, Luo JQ, Marans HY, Wong S, Naddaf SY, El-Zeftawy HM, Omar WS, Mithilesh K, Abujudeh H, Atay S. Fluorine-18-fluorodeoxyglucose double-head gamma camera coincidence imaging of recurrent colorectal carcinoma. *J Nucl Med* 1998; 39:654–656.
12. Luig H, Eschner W, Bähre M, Voth E, Nolte G. An iterative strategy for determining the source distribution in single photon computed tomography using a rotating gamma camera (SPET). *Nucl Med* 1988; 27:140–146.
13. Shuman WP, Baron RL, Peters MJ, Tazioli PK. Comparison of STIR and spin-echo MR imaging at 1.5 T in 90 lesions of the chest, liver, and pelvis. *AJR Am J Roentgenol* 1989; 152:853–859.
14. Bydder GM, Young IR. MR imaging: clinical use of the inversion recovery sequence. *J Comput Assist Tomogr* 1985; 9:659–675.
15. Bertino RE, Porter BA, Stimac GK, Tepper SJ. Imaging spinal osteomyelitis and epidural abscess with short TI inversion recovery (STIR). *AJNR Am J Neuroradiol* 1988; 9:563–644.
16. Gratz S, Braun HG, Behr TM, Meller J, Herrmann A, Conrad M, Rathmann D, Bertagnoli R, Willert HG, Becker W. Photopenia in chronic vertebral osteomyelitis with technetium-99m-antigranulocyte antibody (BW 250/183). *J Nucl Med* 1997; 38:211–216.
17. Sharif HS, Morgan JL, al Shahed MS, al Thagafi MY. Role of CT and MR imaging in the management of tuberculous spondylitis. *Radiol Clin North Am* 1995; 33:787–804.
18. Zhuang H, Duarte PS, Pourdehand M, Shnier D, Alavi A. Exclusion of chronic osteomyelitis with F-18 fluorodeoxyglucose positron emission tomographic imaging. *Clin Nucl Med* 2000; 25:281–284.
19. de Winter F, van de Wiele C, Vogelaers D, de Smet K, Verdonk R, Dierckx RA. Fluorine-18 fluorodeoxyglucose-positron emission tomography: a highly accurate imaging modality for the diagnosis of chronic musculoskeletal infections. *J Bone Joint Surg Am* 2001; 83-A:651–660.
20. Robiller FC, Stumpe KD, Kossmann T, Weisshaupt D, Bruder E, von Schulthess GK. Chronic osteomyelitis of the femur: value of PET imaging. *Eur Radiol* 2000; 10:855–858.
21. Musher DM, Thorsteinsson SB, Minuth JN. Vertebral osteomyelitis – still a diagnostic pitfall. *Arch Intern Med* 1976; 136:105.
22. Tehranzadeh J, Wong E, Wang F, Sadighpour M. Imaging of osteomyelitis in the mature skeleton. *Radiol Clin North Am* 2001; 39:223–250.
23. Kubota R, Yamada S, Kubota K, Ishiwata K, Tamahashi N, Ido T. Intratumoral distribution of fluorine-18-fluorodeoxyglucose in vivo: high accumulation in macrophages and granulation tissues studied by microautoradiography. *J Nucl Med* 1992; 33:1972–1980.
24. Yamada S, Kubota K, Kubota R, Ido T, Tamahashi N. High accumulation of fluorine-18-fluorodeoxyglucose in turpentine-induced inflammatory tissue. *J Nucl Med* 1995; 36:1301–1306.
25. Jones HA, Clark RJ, Rhodes CG, Schofield JB, Krausz T, Haslett C. In vivo measurement of neutrophil activity in experimental lung inflammation. *Am J Respir Crit Care Med* 1994; 149:1635–1639.



26. Guhlmann A, Brecht-Krauss D, Suger G, Glatting G, Kotzerke J, Kinzl L, Reske SN. Chronic osteomyelitis: detection with FDG PET and correlation with histopathologic findings. *Radiology* 1998; 206:749–754.
27. Källicke T, Schmitz A, Risse JH, Arens S, Keller E, Hansis M, Schmitt O, Biersack HJ, Grünwald F. Fluorine-18 fluorodeoxyglucose PET in infectious bone diseases: results of histologically confirmed cases. *Eur J Nucl Med* 2000; 27:524–528.
28. Rigo P, Paulus P, Kaschten BJ, Hustinx R, Bury T, Jerusalem G, Benoit T, Foidart-Willems J. Oncological applications of positron emission tomography with fluorine-18 fluorodeoxyglucose. *Eur J Nucl Med* 1996; 23:1641–1674.
29. Kim EE, Pjura GA, Lowry PA, Gobuty AH, Traina JF. Osteomyelitis complicating fracture: pitfalls of <sup>111</sup>In leukocyte scintigraphy. *Am J Roentgenol* 1987; 148:927–930.